The Role of MASWH in Rooftop Temperature Regulation: An Analysis of Attic and Room Temperatures

Jirasak Pukdum[1], Withaya Puangsombut[2], and Tinnapob Phengpom[3,*]

ARTICLE INFO

Article history:
Received: 19 Septmeber 2023
Revised: 1 July 2024
Accepted: 2 February 2025
Online: 15 May 2026

Keywords:
Mixed asphalt
Solar water heater
Heat gain reduction
Thermo-economic
Attic temperature

ABSTRACT

In this study, the efficacy of the Mixed Asphalt Solar Water Heater (MASWH) integrated on rooftops was systematically assessed for its role in reducing indoor heat gain. Two identical structures, each measuring 1m x1 m x 1m, were employed: one incorporated the MASWH, while the other served as a control. The MASWH was characterized by dimensions of 0.05 m in thickness, 0.5 m in width, and 1 m in length, and was affixed to a roof inclined at 30°. Data analysis revealed a notable temperature reduction in the MASWH-fitted structure: a decrease of 3°C in the attic and 4°C in the room. This reduction represented a 7-10% decrease in overall ambient temperature. Additionally, when evaluating heat gain efficiency, the structure equipped with MASWH surpassed the control by 5-12 Wm^{-2}. Water within the system reached a temperature peak of 52.8°C. The findings underscore the MASWH's potential as an innovative solution to heat transfer challenges. Economically, the system presents a viable option with a payback period of merely 2.5 years, underscoring its practicality in real-world applications.

1. INTRODUCTION

Challenges like global warming and energy scarcity have prompted a worldwide shift in energy policies, spurring interest in renewable energy technologies across nations. Solar power stands as a potential solution, enhancing energy security through the reliance on sustainable energy sources. Among the long-term benefits of harnessing solar energy is the advent of solar water heaters, with flat plate solar collectors being a prevalent choice for domestic heating purposes due to their cost-effectiveness [1]. Numerous studies have sought to enhance the performance of these collectors. For instance, Said et al. [2] demonstrated that TiO_2-H_2O nanofluid as a working medium improved collector efficiency in comparison to water. Michael and Iniyan [3] found that the inclusion of CuO nanoparticles boosted the solar water heaters' efficiency by 6.3% at specific concentrations. Similarly, He et al. [4] showcased that the thermal conductivity of Cu-H_2O nanofluids notably enhanced the flat plate solar collector's efficiency. Additional studies by Jouybari et al. [5] and others indicated that using different nanofluids or modifications like passive air-cooling channels and reflective sheeting can significantly optimize collector efficiency and lifespan. Furthermore, research by Prakasam et al. [6] emphasized the positive impacts of using specialized glass, like Fluorine-doped Tin Oxide (FTO), in solar water heater systems.

Solar water heaters are predominantly installed on rooftops of residences and buildings due to their direct exposure to sunlight. Effective energy utilization in these structures often correlates with intelligent building design, which emphasizes minimizing heat influx. Consequently, there's been a focus on deploying and evaluating tools that curtail heat transfer indoors. Puangsombut et al. [7] explored attic heat gain reduction associated with rooftop solar collectors. Separately, Amornleetrakul et al. [8] introduced the Ventilated Roof Tile (VRT) for tempering heat entry, showcasing its superiority to traditional concrete tiles in experiments using houses with an area of 2.25 m^2. Moreover, Juengpimonyanon et al. [9] employed tile ventilators to mitigate ceiling heat influx, comparing houses with distinct tile types. Subsequently, Phiraphat et al. [10] compared standard PV panels and the PV Roof Solar Collector (PV-RSC), observing a 25% enhancement in PV performance with the latter while also inhibiting heat influx. Prommas et al. [11] further examined how a light-vent pipe, made from aluminum and angled at 30°, impacted heat penetration. This current research probes the potential of integrating MASWH on rooftops to reduce heat gain, also delving into its economic viability by anticipating the payback duration.

[1]*Faculty of Architecture and Design, Rajamangala University of Technology Rattanakosin, Salaya, Nakhon Pathom, 73170, Thailand.*
[2] *Rattanakosin College for Sustainable Energy and Environment (RCSEE),96 Moo3, Phuttamonthon 5 Road, Salaya, Nakhon Pathom, 73170, Thailand.*
[3]*Institute for innovative learning, Mahidol University, 999 Phuttamonthon 4 Road, Salaya, Nakhon Pathom, 73170, Thailand.*
**Corresponding author:* Tinnapob Phengpom; Phone: +66-(0)94-573-4464; Email: tinnapob.phe@mahidol.ac.th.

2. RESOURCES AND PROCEDURES

2.1 Description and setup of the experiment

The layout and design of the MASWH are shown in Figure 1. The top glass covers of this heater measures 0.04 meters in diameter. The glass cover and the mixed asphalt below are separated by a 0.05 m air gap. The selective collector is made of mixed asphalt and measures 0.05 m in thickness, 0.5 m in breadth, and 1 m in length. A 9-meter-long, serpentine-style copper pipe with an internal diameter of 0.0952 meters is buried about 3/4 of the way through the mixed asphalt. The layer of insulation is 0.01 m thick.

Two comparable miniature windowless dwellings were built in order to measure the reduction in heat gain. The experimental house incorporated the MASWH on its roof, while the counterpart served as a reference, as depicted in Figures 3 and 4. Water was channeled into the MASWH at a rate of 0.02 kg per second. Both houses were steel-framed, featuring roofs made of corrugated metal sheets, covering an area of 1.4x1.60 m (2.24 m^2) set at a 30° tilt. The ceiling, constructed from gypsum board, had a thickness of 0.09 m. Rooms measured 1x1 m (1 m^2) with a height of 1 m. Walls were lined with a 0.01 m-thick smart board, and every wall, both inside and out, was painted white. Notably, the attic and room lacked ventilation openings.

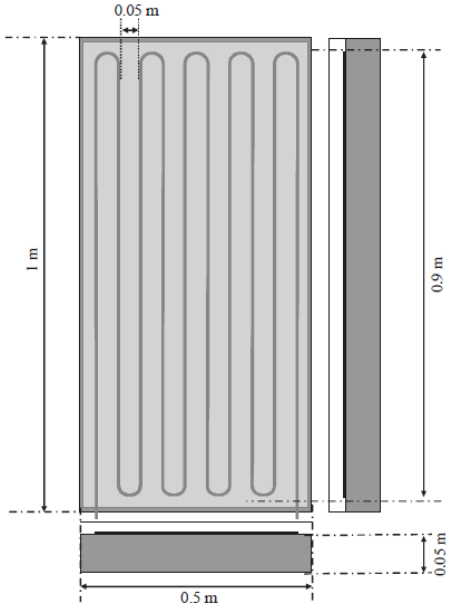

Fig. 1. Mixed asphalt solar water heater dimension

A pyranometer (Kipp and Zonen, Model: CMP11, with a range of 310-2800 μm and an uncertainty of less than 2%) was set up on the rooftop to gauge solar radiation levels. We utilized a flow meter (Nitto, Model: Z-5015, with an accuracy of ±5%) to determine the volume flow rate. For temperature measurements, K-type thermocouples (with a range of 0-800 ºC and an accuracy of ±0.4 ºC) were linked to a data logger (Hioki, Model: LR8422-20, with an accuracy of ±0.7%). Additionally, a heat flux sensor (EKO flow meter: Model MF-180, with a range of 1-1400 Wm^{-2} and an accuracy of ±2%) was employed to assess heat gain, as depicted in Figures 2 and 3. Data collection occurred from 6:00 to 18:00, with readings taken every minute. The test structures were situated on the rooftop of the Faculty of Architecture and Design at Rajamangala University of Technology Rattanakosin, Thailand, positioned at latitude 13°47'41.3"N and longitude 100°17'56.7" E.

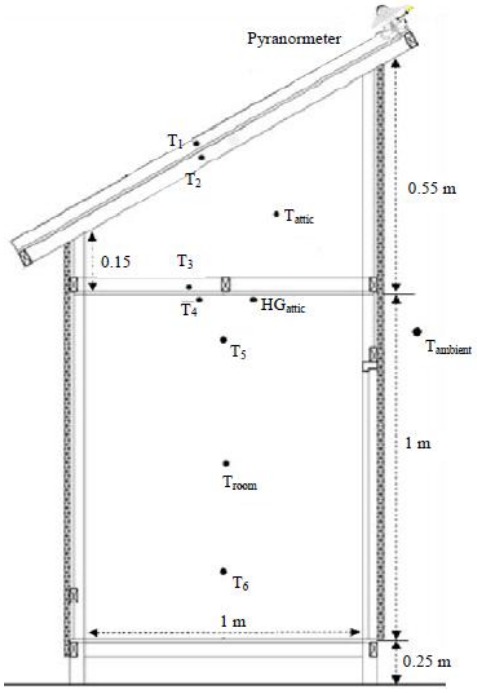

Fig. 2. Schematic of reference house

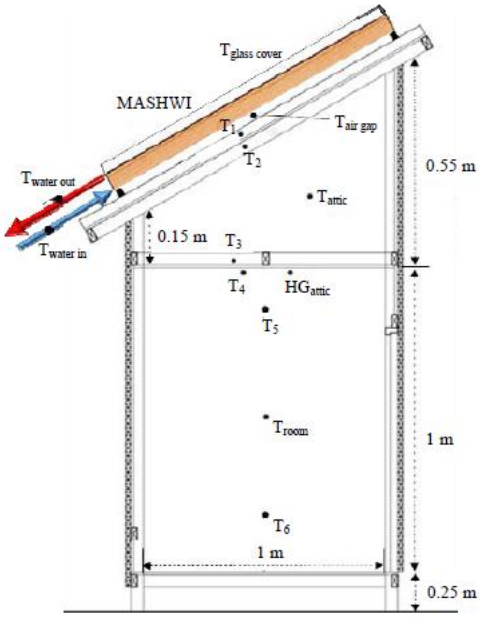

Fig. 3. Schematic of house with MASWH.

2.2. Data reduction

The energy efficiency of the MASWH is determined through an energy balance, which outlines the portion of the incoming solar radiation that is converted into useful energy. This useful energy is represented by the collector, with the subsequent. The fluid's heat gain is defined as:

$$Q_u = A_c F_R [S-U_L (T_{pm}-T_a)] = \dot{m} C_p(T_{fo} -T_{fi}) \quad (1)$$

where:

Q_u : Useful energy gain [W]
A_c : Collector area [m^2]
F_R : Collector heat removal factor [-]
S : Solar radiation absorbed per unit area [$W.m^{-2}$]
U_L : Collector overall heat loss coefficient [$W.m^{-2}$]
T_{pm} : The mean of absorber plate temperature [°C]
T_a : Ambient temperature [°C]
$\dot{m}$: Mass flow rate [$kg.s^{-1}$]
C_p : The specific heat of water [$kJ.kg.s^{-1}$]
T_{fi} : The fluid inlet temperature [°C]
T_{fo} : The fluid outlet temperature [°C].

3. DISCUSSION AND RESULTS

3.1 Ambient temperature and Solar radiation

The study assessed the efficacy of a rooftop-integrated MASWH in mitigating heat gain, aiming to reduce energy consumption within rooms. For the experiment, days with clear skies were chosen during March to April 2023, which is the summer season. The conditions of the environment and solar radiation were specifically chosen to optimize results, as illustrated in Fig. 4.

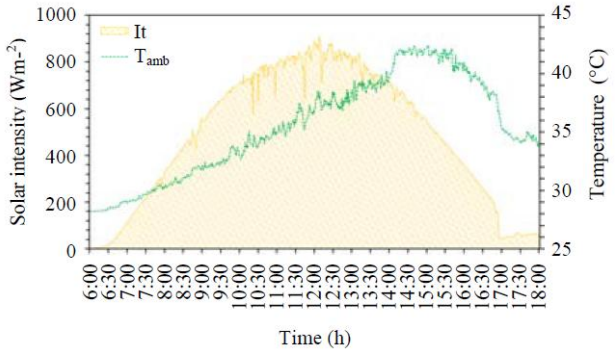

Fig. 4. Fluctuation in solar intensity and ambient temperature.

As depicted in Fig. 4, the solar intensity at a 30° angle and ambient temperature during the day (from 6:00 to 18:00) are presented. Clearly, on a day with clear skies, solar intensity rose steadily from 06:00 until 12:30, after which it began to decline until 17:00. In a similar pattern, ambient temperature ascended from 06:00 to 14:30 and then started to fall until 17:00. By 17:00, both solar radiation and ambient temperature experienced a sharp drop due to light cloud cover and a sprinkle of rain. The peak solar intensity reached 910 Wm^{-2} at 12:10, coinciding with an ambient temperature of 37.9°C. The highest ambient temperature recorded was 42.5°C at 14:50, when the solar intensity was 531.6 Wm^{-2}. The average solar intensity and ambient temperature were 490 Wm^{-2} (or 21.28 MJm^{-2} per day) and 34.8°C, respectively. The settings were perfect for this investigation because of the experimental area's high average sun radiation and ambient temperature.

3.2 Attic temperature

Figure 5 illustrates the hourly fluctuations in attic temperature between the house equipped with MASWH and the standard house. Throughout the day, the roof absorbs solar energy, which then causes heat to build up in the attic. Both houses showed similar attic temperatures in the morning, as this is when heat begins to accumulate in this space. However, as solar intensity and ambient temperatures rose, differences became evident. The normal home and the MASWH-equipped house attained peak attic temperatures of 46.5°C and 44.5°C, respectively. The ordinary house's attic temperature was 1.5°C higher on average than the MASWH-equipped house's. The MASWH-equipped house demonstrated superior heat reduction in the attic, especially between the hours of 7:00 and 17:00. This is attributed to the MASWH intercepting direct solar radiation, preventing it from reaching the roof directly. As evening approached and ambient temperatures began to drop, heat stored in the attic began to dissipate, influenced by the roof's heat transfer characteristics.

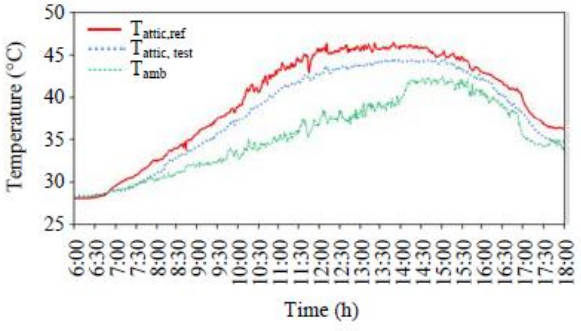

Fig. 5. Fluctuation in attic and ambient temperatures.

3.3 Ceiling temperature

The top surface of the ceiling (facing the attic) is directly exposed to the heat from the attic throughout the day. As shown in Figure 6, the temperatures of these ceiling surfaces in both houses steadily rose in tandem with the ambient temperature, peaking at 45 °C and 43 °C around 14:15 and 14:20 respectively. Interestingly, the reference home's ceiling temperature was always higher than that of the

MASWH-integrated house. This occurred as a result of the reference house's ceiling retaining heat all day. The temperature difference between the two houses ranged from 1 to 2.7 °C between 6:00 and 17:00. Subsequently, as the day wore on, the ceiling temperatures in both houses began to decline, dissipating heat to the surroundings in a manner comparable to the attic temperatures.

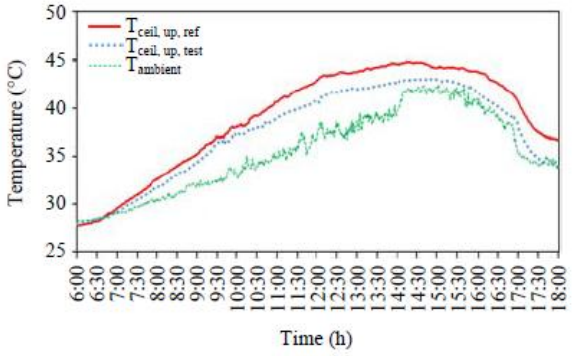

Fig. 6. Change in top-side ceiling and ambient temperatures.

Figure 7 displays the temperatures of the ceilings' underside (facing the room). The trend observed for the underside ceiling temperatures in both houses mirrored that of the upper side, primarily because heat was continuously transferred from the top surface to the underside throughout the day. Concurrently, the underside ceiling of the reference house retained and slowly increased its heat. At its peak, the temperature of the underside ceiling in the house integrated with MASWH was 2.5°C cooler than in the reference house, observed at 16:20. This underscores the effectiveness of the MASWH in reducing heat transmission from the ceiling into the room.

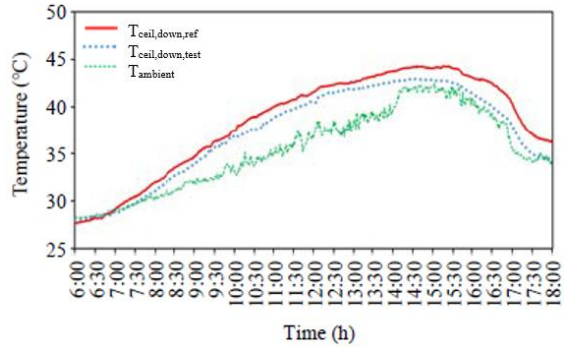

Fig.7. Change in underside ceiling and ambient temperatures.

3.4 Room temperature

Figure 8 displays the temperature variations in the two rooms. Solar radiation impacts the rooftop, leading to heat buildup in the attic, which then permeates through the ceiling into the non-ventilated rooms throughout the day. Notably, the reference house's room temperature followed a similar pattern as the ambient temperature. However, its average temperature remained consistently higher than the room with the MASWH integration. The most notable temperature difference between the MASWH-integrated house and the reference house was 4 °C. Furthermore, between 14:10 and 16:30, the room with MASWH had temperatures ranging from 0.1 to 0.7 °C below the ambient. This aligns with the inclusion of MASWH on the rooftop. Evidently, the results suggest that MASWH effectively mitigates heat buildup in the room via the ceiling and attic.

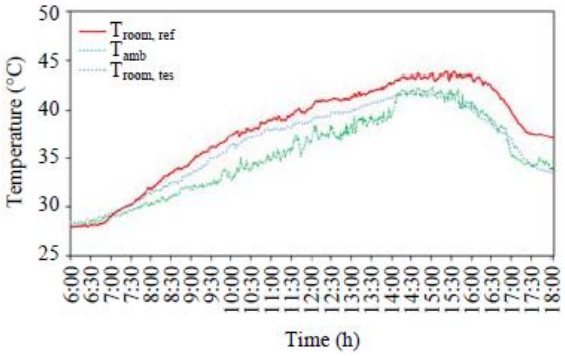

Fig. 8. Fluctuation between room and ambient temperatures.

3.5 Heat gain and decrease of heat gain

Heat transmission was observed in both the MASWH-integrated house and the reference house via the ceiling. This was monitored using a heat flux sensor positioned at the center of the ceiling's underside (facing the room). Figure 9 illustrates the heat gain percentages and their reduction. The MASWH-integrated house demonstrated a heat gain reduction of 5-12 Wm^{-2} compared to the reference house, with the daily effective period showing a heat gain reduction ranging between 20-85%. This confirms that integrating the MASWH on the rooftop can more effectively mitigate heat transfer through the ceiling than in the standard reference house.

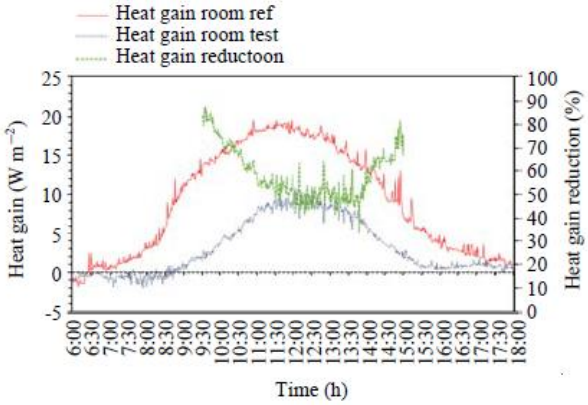

Fig. 9. Changes in heat gain and decrease in heat gain.

3.6 Water temperature

In this research, the experiment focused on examining the water temperature when feeding water from an external source into a collector at a flow rate of 0.02 kg/sec. The

temperature details can be found in Fig. 10. The temperature was notably lower in the morning, then it rose significantly, reaching its peak before gradually falling in the afternoon. This change correlates with daily variations in solar radiation and ambient temperature. The highest recorded outlet water temperature was 52.8°C at 12:53, with a maximum temperature difference of 14.8°C between the inlet and outlet. On average, there was an 8.4°C difference between the daily inlet and outlet water temperatures.

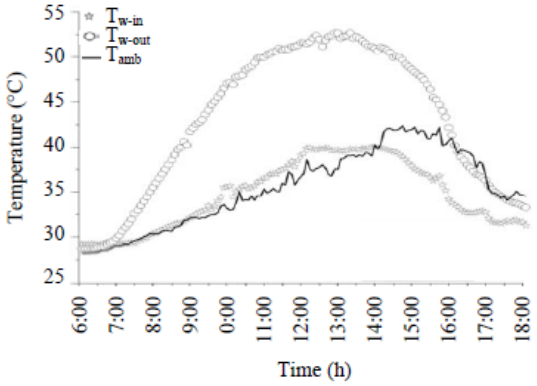

Fig. 10. Temperature variations at the water's inflow, output, and ambient.

3.7 Useful energy

Figure 11 illustrates the beneficial energy derived from the collector between 7:00 and 17:00, ranging from 115-320 Wm^{-2}, while the solar intensity varies between 120-900 Wm^{-2}. The effective energy for MASWH lies between 30-36%. Notably, the trend of useful energy mirrors that of the solar intensity.

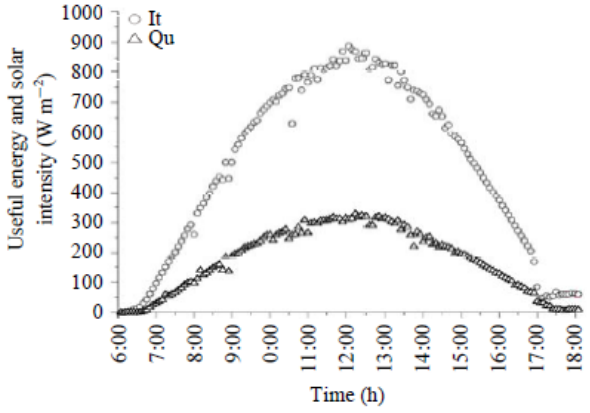

Fig. 11. Useful energy

3.8 Economic evaluation

To evaluate the economic benefits of the MASWH, it was positioned on the testing house's rooftop. Using the first law of thermodynamics, an energy balance was conducted from the roof to the ceiling to determine the heat load entering the room. Figures 6 and 7 display the energy balance for the attic. The subsequent assumptions were made for the analysis:

- Heat transfer through the attic occurs under transient conditions.
- There's no ventilation in the attic system
- Heat accumulation from walls and floor is overlooked.
- The water's flow rate remains consistent.

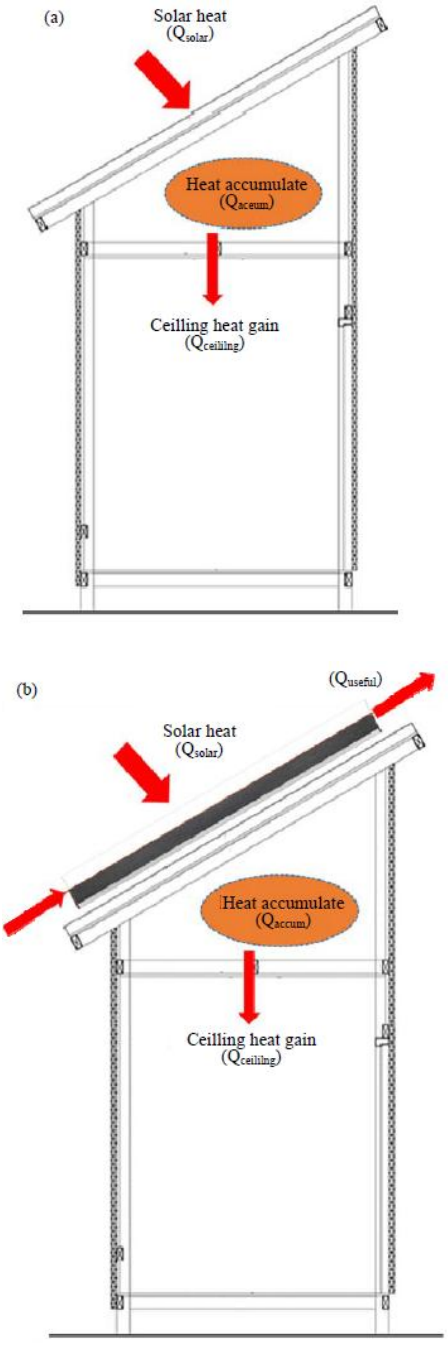

Fig. 12. (a) The reference home and (b) the house with MASWH incorporated on the roof.

It can also demonstrate that:

$$Q_{ceiling} = Q_{solar} - Q_{accum} \quad (2)$$

Equation 3 may be used to represent the energy balance for dwellings integrated with MASWH (Fig. 12b):

$$Q_{ceiling} = Q_{solar} - Q_{useful} - Q_{accum} \quad (3)$$

where:

Q_{solar} : Heat produced by solar radiation [W]

Q_{accum} : Heat builds up in the attic [W]

Q_{useful} : Useful energy [W]

$Q_{ceiling}$: Heat builds up toward the ceiling [W]

To assess the potential energy reductions in air-conditioning and electric water-heating systems for residences equipped with MASWH, an energy-savings analysis was undertaken. The evaluation employed a conventional indoor temperature set-point of 26 °C for air-conditioned spaces, which is representative of typical residential conditions in Thailand. At this set-point, the daily electricity consumption of the air-conditioning unit was determined to be 6.28 kWh. According to Lertsatitthanakorn et al. [12], each 1 °C change in the mean indoor temperature yields an estimated 6.14% decrease in electricity use.

Experimental observations indicated that the average ceiling heat gains for the MASWH-equipped dwelling and the reference dwelling were 14 W and 5.4 W, respectively. Over a full day, the mean beneficial energy reached 254 W. These heat-gain and beneficial-energy values correspond to equivalent electrical power levels of 14 W, 5.4 W, and 254 W, respectively.

The total estimated cost of the MASWH system is 2,660 Baht, which includes expenses for construction, asphalt mixture, copper tubing, the glass cover, and other associated materials. The payback period refers to the length of time required for the system's accumulated energy savings to offset the initial investment. This period can be determined using the calculation presented in Eq. 4, following the method described by Sarachitti et al. [13].

$$P = B\left[\frac{(1+r)^n - 1}{r(1+r)^n}\right] \quad (4)$$

where:

P : The price of the MASWH

B : Energy-efficient electric heating of water

R : Rate of interest

Thailand's tropical climate is characterized by distinct seasonal patterns, with the winter period occurring from November to January and the summer season extending from February to May, as reported by Lertsatitthanakorn et al. [12]. Consequently, the MASWH system operates predominantly during these winter and summer intervals. It operates for 8 hours daily (from 9:00 to 16:00) and 210 days annually. In homes equipped with MASWH, the room temperature is typically 1°C to 4°C cooler than in reference rooms. As a result, there's an energy saving of 47 kWh/year for air conditioning. Additionally, there's an electrical energy saving of 213 kWh/year for water heating. It's evident that the temperature set-point has a minimal impact on the payback period, mainly because the energy savings from water heating significantly outweigh those from air conditioning. On average, the electricity cost from the Electricity Generating Authority of Thailand (EGAT) is 4.217 Baht/kWh, and the Thai bank's interest rate is roughly 6.2%. Hence, the MASWH yields an annual power savings of 260 kWh, which translates to a monetary saving of 1,094.5 baht each year. The investment recoups itself in 2.5 years.

4. CONCLUSION

The capability of the Mixed Asphalt Solar Water Heater (MASWH) to attenuate thermal gains was examined through controlled experimental testing. The investigation employed two instrumented test structures: one incorporating the MASWH on its roof assembly and a second baseline structure used to quantify comparative heat-gain reductions. Analysis of the measured thermal performance yielded the following results:

1. The attic temperature in the house equipped with MASWH was consistently 1-1.5 °C (or 0-5% in range) cooler than the reference house.
2. The upper ceiling temperature of the MASWH house was reduced by 0.2-2.7°C compared to the reference house. Similarly, the lower ceiling temperatures in both homes followed the same pattern.
3. The maximum temperature reduction on the underside of the MASWH house's ceiling was 2.5 °C, a result of the lower heat gains from the attic compared to the reference house.
4. The MASWH house's room temperature was 4 °C cooler than the reference house, a decline of about 10%.
5. The house featuring MASWH experienced a heat gain reduction ranging between 1.2-10 Wm^{-2}, or 20-85% during optimal operation times.
6. Observations revealed that both the ceiling and room temperatures, as well as heat gains in the MASWH house, were reduced compared to the reference house. This is attributed to the MASWH system's ability to deflect direct solar rays from the roofing structure and absorb the roof's heat. This suggests that MASWH can effectively reduce the heat influx inside homes and decrease energy use when integrated on rooftops.

7. The temperature disparity between the water inlet and outlet was 14.8 °C, with the highest outlet water temperature reaching 52.8 °C. The beneficial energy fluctuated between 115-320 Wm^{-2}.
8. Economic evaluations determined a payback period of 2.5 years for MASWH. Given its potential for leveraging renewable solar energy and promoting energy conservation, it's recommended that MASWH be adopted for residential buildings' rooftops.

ACKNOWLEDGEMENTS

The research team expresses their appreciation to the Faculty of Architecture and Design at Rajamangala University of Technology Rattanakosin (RMUTR) and the Institute for Innovative Learning at Mahidol University for their financial contribution to this study.

REFERENCES

[1] Shah, Y.T. 2018. Thermal Energy: Sources, Recovery and Applications. 1st Edn., CRC Press, Raton, Florida: CRC Press.

[2] Said, Z.; Sabiha, M.A.; Saidur, R.; Hepbasli, A.; Rahim, N.A.; Mekhilef, S.; and Ward, T.A. 2015. Performance enhancement of a flat plate solar collector using titanium dioxide nanofluid a polyethylene glycol dispersant. Journal of Cleaner Production. 92: 343-353.

[3] Michael, J.J.; and Iniyan, S. 2015. Performance of copper oxide/water nanofluid in a flat plate solar water heater under natural and forced circulations. Energy Conversion and Management. 95(1): 160-169.

[4] He, Q.; Zeng, S.; and Wang, S. 2015. Experimental investigation on the efficiency of flat-plate solar collectors with nanofluids. Applied Thermal Engineering.88: 165-171.

[5] Jouybari, H.J.; Saedodin, S.; Zamzamian, A.; and Nimvari, M.E.2017. Experimental investigation of thermal performance and entropy generation of a flat-plate solar collector filled with porous media. Applied Thermal Engineering. 127: 1506-1517.

[6] Prakasam, M.J.S.; Vellingiri, A.T.; and Nataraj, S. 2017. An experimental study of the mass flow rates effect on flat-plate solar water heater performance using Al2o3/water nanofluid. Thermal Science. 21(2): 379-388.

[7] Puangsombut, W.; Hirunlabh, J.; Khedari, J.; Zeghmati, B.; and Win, M.M. 2007. Enhancement of natural ventilation rate and attic heat gain reduction of roof solar collector using radiant barrier. Building and Environment. 42(6): 2218-2226.

[8] Amornleetrakul, O.; Puangsombut, W.; and Hirunlabh, J. 2014. Field investigation of the small house with the ventilated roof tiles. Advanced Materials Research 931: 1233-1237.

[9] Juengpimonyanon, K.; Puangsombut, W.; and Ananacha, T. 2014. Field investigation on thermal performance of the tile ventilator. Applied Mechanics and Materials. 619: 73-77.

[10] Phiraphat, S.; Prommas, R.; and Puangsombut, W. 2017. Experimental study of natural convection in PV roof solar collector. International Communications in Heat and Mass Transfer. 89 (1): 31-38.

[11] Prommas, R.; Phiraphat, S.; and Rattanadecho, P. 2019. Energy and exergy analyses of PV roof solar collector. International Journal of Heat and Technology. 37: 303-312.

[12] Lertsatitthanakorn, C.; Atthajariyakul, S.; and Soponronnarit, S. 2009. Techno-economical evaluation of a Rice Husk Ash (RHA) based sand-cement block for reducing solar conduction heat gain to a building. Construction and Building Materials. 23(1): 364-369.

[13] Sarachitti, R.; Chotetanorm, C.; Lertsatitthanakorn, C.; and Rungsiyopas, M. 2011. Thermal performance analysis and economic evaluation of roof-integratedsolar concrete collector. Energy and Buildings. 43(6): 1403-1408.